Semi-Analytical Model of Charge Image Formation in Electrophotography

Brandon A. Kemp; Arkansas State University; Jonesboro, Arkansas/USA

Abstract

High resolution latent image formation is an important step in electrophotography to achieve high quality prints. Presently, analytical models exist for the other important steps: photoconductor charging, development (both single and dual component), and transfer. We present here an analytical model of charge image generation on the surface of an organic photoconductor due to laser exposure. The inputs to the model include laser intensity profile as a function of time, quantum efficiency of the charge generation layer, hole mobility of the charge transport layer, and initial charge density on the surface of the PC. The output of the model is the PC surface charge map as it evolves in time, which is a key input to the toner development process in electrophotography.

Introduction

Analytical modeling of engineering systems provides advantages of rapid conceptual iteration, low cost concept evaluation, and detailed physical understanding. Analytical models exists for other critical steps important to achieve high resolution image formation in electrophotography, such as charging, development, and transfer. Here, an analytical model for charge image formation on a photoconductor (PC) surface due to laser exposure is presented.

Mathematical Model

The charge transport model implemented here is an analytical model updated with finite difference approximations in time. The charge and field solutions are continuous solutions obeying Maxwell's equations [3]. A diagram of the mathematical model is shown in Figure 1.

Charge Continuity

Continuity equations for energy, momentum, and charge result directly from Maxwell's equations. Of interest here, is the charge conservation condition which describes the transport of holes in the PC [1]

$$\frac{\partial \rho(\bar{r},t)}{\partial t} = -\nabla \cdot \bar{J}(\bar{r},t) = -\nabla \cdot [\mu \rho(\bar{r},t)\bar{E}(\bar{r},t)], \tag{1}$$

where $\bar{r} = x\hat{x} + y\hat{y} + z\hat{z}$ is the position vector, ρ is the hole charge density, $\bar{J}$ is the free hole current density, μ is the hole mobility, and $\bar{E}$ is the local electric field. It is assumed that disassociated electrons are drained to the PC core. Applying the chain rule of differentiation yields

$$\frac{\partial \rho(\bar{r},t)}{\partial t} = -\mu \rho(\bar{r},t)\nabla \cdot \bar{E}(\bar{r},t) - \mu \bar{E}(\bar{r},t) \cdot \nabla \rho(\bar{r},t). \tag{2}$$

Taking a finite-difference approximation to the time derivative yields the an update equation at each time step,

$$\Delta\rho = -\Delta t \mu \left[\rho(\bar{r},t)\nabla \cdot \bar{E}(\bar{r},t) + \bar{E}(\bar{r},t)\nabla\rho(\bar{r},t)\right]. \tag{3}$$

Charge Expansion

The volume charge at each time step is expanded in a three-dimensional (3-D) Fourier series

$$\rho(x,y,z) = \sum_{m=0}^{M}\sum_{n=0}^{N}\sum_{p=1}^{P} \alpha_{mnp}\cos(k_m x)\cos(k_n y)\sin(k_p z), \tag{4}$$

where

$$k_m = \frac{m\pi}{a}, \qquad k_n = \frac{n\pi}{b}, \qquad k_p = \frac{p\pi}{2h} \tag{5}$$

and the constants α_{mnp} are determined in the first time step by mode matching with the input charge. At each subsequent time step the Fourier coefficients are updated from the charge update equation.

The PC surface charge is likewise expanded in a two-dimensional (2-D) Fourier series

$$\rho_s(x,y) = \sum_{m=0}^{M}\sum_{n=0}^{N} \beta_{mn}\cos(k_m x)\cos(k_n y), \tag{6}$$

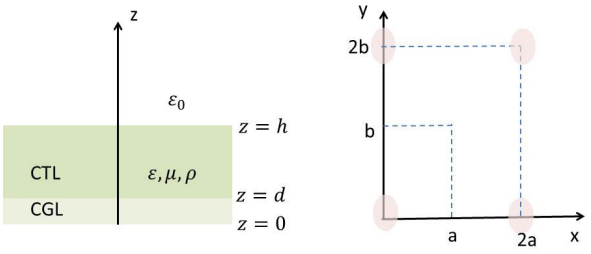

Figure 1. *Diagram showing the mathematical model in the $z-\rho$ plane and the $x-y$ plane. The CGL layer extends from $0 < z < d$, the CTL layer extends from $d < z < h$, and air occupies the region $z > h$. For simplicity, the CTL and CGL have the same dielectric permittivity ε and hole mobility μ. In the $x-y$ plane, the domain is repeated with a period of $2a$ in the x-direction and a period of $2b$ in the y-direction due to the Fourier expansion.*

where the constants β_{mn} are determined in the first time step by mode matching with the input surface charge. At each subsequent time step, the surface charge Fourier coefficients are updated from the charge update equation applied at the $z = h$ boundary.

Field Solution

The fields in each region satisfy the Maxwell equations. The electric potential in Region I ($0 < z < h$) is determined from the Poisson equation, and the potential in Region II ($z > h$) is determined from the Laplace equation. The potentials are

$$\Psi^{(I)}(x,y,z) = \sum_{m=0}^{M}\sum_{n=0}^{N}\cos(k_m x)\cos(k_n y)\left[B_{mn}^{(1)}\sinh(k_z z) + \sum_{p=1}^{P}A_{mnp}\sin(k_p z)\right] + K_1 z \quad (7a)$$

$$\Psi^{(II)}(x,y,z) = \sum_{m=0}^{M}\sum_{n=0}^{N}\cos(k_m x)\cos(k_n y)B_{mn}^{(2)}e^{-k_z z}, \quad (7b)$$

where $B_{mn}^{(1)}$, $B_{mn}^{(2)}$, and K_1 are determined from the boundary conditions. The Poisson equation requires that

$$k_z = \sqrt{k_m^2 + k_n^2} \quad (8)$$

and

$$A_{mnp} = \frac{\alpha_{mnp}}{\varepsilon\varepsilon_0}\left[k_m^2 + k_n^2 + k_p^2\right]^{-1}. \quad (9)$$

The electric field is defined as $E(\bar{r},t) = -\nabla\Psi(\bar{r},t)$. In Region I the electric field is

$$E_x^{(I)}(x,y,z) = \sum_{m=0}^{M}\sum_{n=0}^{N}k_m\sin(k_m x)\cos(k_n y) \times \left[B_{mn}^{(1)}\sinh(k_z z) + \sum_{p=1}^{P}A_{mnp}\sin(k_p z)\right] \quad (10a)$$

$$E_y^{(I)}(x,y,z) = \sum_{m=0}^{M}\sum_{n=0}^{N}k_n\cos(k_m x)\sin(k_n y) \times \left[B_{mn}^{(1)}\sinh(k_z z) + \sum_{p=1}^{P}A_{mnp}\sin(k_p z)\right] \quad (10b)$$

$$E_z^{(I)}(x,y,z) = -\sum_{m=0}^{M}\sum_{n=0}^{N}\cos(k_m x)\cos(k_n y)\left[k_z B_{mn}^{(1)}\cosh(k_z z) + \sum_{p=1}^{P}k_p A_{mnp}\cos(k_p z)\right] - K_1, \quad (10c)$$

and in Region II the electric field is

$$E_x^{(II)}(x,y,z) = \sum_{m=0}^{M}\sum_{n=0}^{N}B_{mn}^{(2)}k_m\sin(k_m x)\cos(k_n y)e^{-k_z z} \quad (11a)$$

$$E_y^{(II)}(x,y,z) = \sum_{m=0}^{M}\sum_{n=0}^{N}B_{mn}^{(2)}k_n\cos(k_m x)\sin(k_n y)e^{-k_z z} \quad (11b)$$

$$E_z^{(II)}(x,y,z) = \sum_{m=0}^{M}\sum_{n=0}^{N}B_{mn}^{(2)}k_z\cos(k_m x)\cos(k_n y)e^{-k_z z}. \quad (11c)$$

Boundary Conditions

The field solutions have been chosen carefully so that the potential at the PC core is zero (*i.e.* $V_{core} = \Psi^{(I)}(z=0) = 0$) for simplicity. One could offset the entire solution by a constant value without changing the results of the simulation. The remaining boundary conditions are

$$\Psi^{(II)}(x,y,h) - \Psi^{(I)}(x,y,h) = 0 \quad (12a)$$

$$E_z^{(II)}(x,y,h) - \varepsilon E_z^{(I)}(x,y,h) = \rho_s/\varepsilon_0. \quad (12b)$$

For the $m = 0$,$n = 0$ terms, this yields the values for K_1 and $B_{00}^{(2)}$

$$K_1 = \frac{\beta_{00}}{\varepsilon\varepsilon_0} - \sum_{p=1}^{P}A_{00p}k_p\cos(k_p h) \quad (13a)$$

$$B_{00}^{(2)} = K_1 h + \sum_{p=1}^{P}A_{00p}\sin(k_p h). \quad (13b)$$

Note that $B_{00}^{(1)}$ does not contribute to the model and is not considered an unknown of interest. For all other values of m and n, the unknowns are solved algebraically as a 2×2 system

$$a_{11}B_{mn}^{(1)} + a_{12}B_{mn}^{(2)} = b_1 \quad (14a)$$

$$a_{21}B_{mn}^{(1)} + a_{22}B_{mn}^{(2)} = b_2, \quad (14b)$$

where

$$a_{11} = \sinh(k_z h) \quad (15a)$$

$$a_{12} = -e^{-k_z h} \quad (15b)$$

$$a_{21} = \varepsilon k_z\cosh(k_z h) \quad (15c)$$

$$a_{22} = k_z e^{-k_z h} \quad (15d)$$

$$b_1 = -\sum_{p=1}^{P}A_{mnp}\sin(k_p h) \quad (15e)$$

$$b_2 = \frac{\beta_{mn}}{\varepsilon_0} - \varepsilon\sum_{p=1}^{P}A_{mnp}k_p\cos(k_p h). \quad (15f)$$

Discussion

For illustration, a 1-D simulation was run to demonstrate charge spreading in the z-direction. Figure 2 shows a distribution of charge contained in the CGL layer at $t = 0$ and at $t = 30\ \mu s$. The figure shows that the charge has moved toward the surface of the PC and spread along the z-axis as the holes migrate toward the surface.

Three dimensional (3-D) simulations take some computational effort. However, typical laser spots can be modeled in the $x-y$ plane with a small number of modes. Figure 3 shows one quadrant of a typical laser profile with up to $M = N = 5$ Fourier expansion representations of the 2-D profile. The coefficients α_{mnp} of the modes are determined by mode matching with the input laser profile mapped to a volume charge density using the smooth z profile in the CGL shown in Figure 2 and the experimentally determined quantum efficiency.

Acknowledgements

The author would like to acknowledge helpful discussions with Julie Whitney and Jon Whitney of Lexmark.

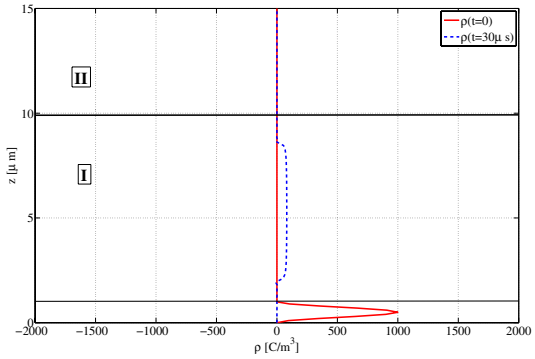

Figure 2. *1-D simulation with $N = 0$, $M = 0$, and $P = 200$. The initial surface charge on the PC is $-50\ nC/cm^2$.*

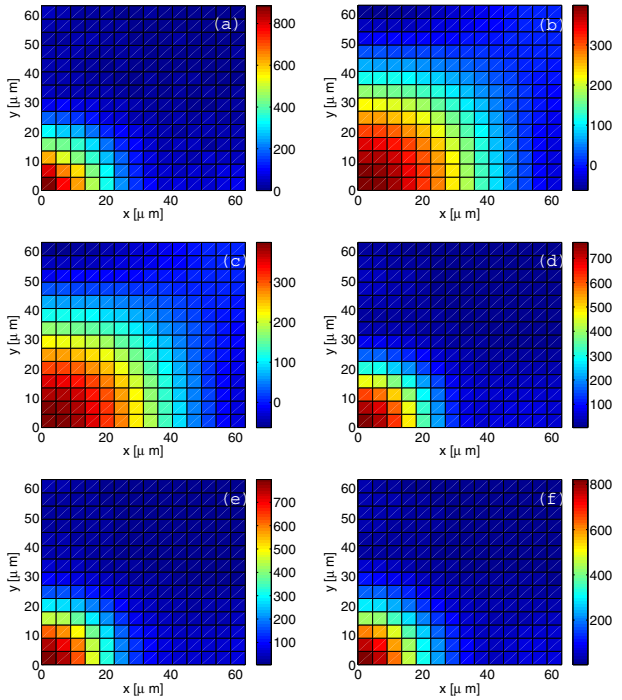

Figure 3. *Mapping of a typical laser profile (a) in one quadrant to Fourier mappings with (b) $M = N = 1$, (c) $M = N = 2$, (d) $M = N = 3$, (e) $M = N = 4$, and (f) $M = N = 5$ modes in x and y. $P = 40$ in each case and the z profile is shown in Figure 2 at $t = 0$.*

References

[1] G. A. Buxton and N. Clarke. Computer simulation of polymer solar cells. *Modelling Simul. Mater. Sci. Eng.*, 15, pg. 13-26, 2007.

[2] Y. Watanabe, H. Kawamoto, H. Shoji, H. Suzuki, and Y. Kishi. A numerical study of high resolution latent image generation by laser beam exposure. *IS&T NIP 16: 2000 International Conference on Digital Printing Technologies*, pg. 822-826, 2000.

[3] M. Panofsky and W. K. H. Philips. *Classical Electricity and Magnetism* (Addison-Wesley, 1964).

Author Biography

Brandon Kemp received his PhD from the Massachusetts Institute of Technology (2007), his MSEE from the University of Missouri-Rolla (1998), and his BSEngr from Arkansas State University (1997). Dr. Kemp is an NSF CAREER award winner and a faculty member in the College of Engineering at Arkansas State University. He previously spent eight years as an R&D engineer with Lexmark International, Inc.